Article

PNP Hydrogel Prevents Formation of Symblephara in Mice After Ocular Alkali Injury

Aditi Swarup[1], Abigail K. Grosskopf[2], Lindsay M. Stapleton[2], Varun R. Subramaniam[1], BaoXiang Li[1], Irving L. Weissman[3], Eric A. Appel[2], and Albert Y. Wu[1]

[1] Department of Ophthalmology, Stanford University School of Medicine, Palo Alto, CA, USA
[2] Department of Materials Science and Engineering, Stanford University, Palo Alto, CA, USA
[3] Institute of Stem Cell Biology and Regenerative Medicine, Stanford University School of Medicine, Palo Alto, CA, USA

Correspondence: Albert Y. Wu, Byers Eye Institute, Department of Ophthalmology, Stanford University School of Medicine, 2452 Watson Court, MC 5353, Palo Alto, CA 94305, USA.
e-mail: awu1@stanford.edu

Purpose: To create an alkali injury symblephara mouse model to study conjunctival fibrosis pathophysiology and test polymer nanoparticle (PNP) hydrogel as a preventative therapeutic.

Methods: Mice were injured using NaOH-soaked filter paper to determine the optimal NaOH concentration to induce the formation of symblephara. Injured mice were observed for 7 days to detect the formation of symblephara. Forniceal shortening observed on hematoxylin and eosin (H&E)-stained tissue sections was used as a symblephara marker. Alpha-smooth muscle actin (α-SMA) expression, Masson's trichrome assay, and periodic acid–Schiff (PAS) staining were used to determine myofibroblast expression, collagen deposition, and goblet cell integrity. PNP hydrogel, with multivalent, noncovalent interactions between modified biopolymers and nanoparticles, was applied immediately after alkali injury to determine its ability to prevent the formation of symblephara.

Results: Forniceal shortening was observed in H&E images with 1N NaOH for 2 minutes after 7 days without globe destruction. PNP hydrogel prevented forniceal shortening after alkali injury as observed by H&E histology. α-SMA expression and collagen deposition in eye tissue sections were increased in the fornix after injury with 1N NaOH compared with uninjured controls. PNP hydrogel treatment immediately after injury reduced α-SMA expression and collagen deposition in the forniceal region. Mucin-secreting goblet cells stained with PAS were significantly lower in alkali-injured and PNP hydrogel–treated conjunctivas than in uninjured control conjunctivas.

Conclusions: We observed that 1N NaOH for 2 minutes induced maximal forniceal shortening and symblephara in mice. PNP hydrogel prevented forniceal shortening and conjunctival fibrosis after injury. This first murine model for symblephara will be useful to study fibrosis pathophysiology after conjunctival injury and to determine therapeutic targets for cicatrizing diseases.

Translational Relevance: This mouse model of symblephara can be useful for studying conjunctival scarring disease pathophysiology and preventative therapeutics. We tested PNP hydrogel, which prevented the formation of symblephara after injury.

Introduction

Each year in the United States, 2.4 million ocular injuries occur, of which 11.5% to 22.1% are due to alkali burns.[1,2] These injuries often lead to ocular scarring and vision loss, with lifelong decreased quality of life, lower economic productivity, and chronic neuropathic pain.[3] Alkali injuries cause conjunctival inflammation, and the resultant fibrosis may cause adhesions between the eyelid and globe, known as symblephara.[4] Symblephara are one of the most challenging eye problems faced by physicians and are debilitating for patients. Alkali burns are more

1

damaging than acid burns, as alkali causes fatty acid saponification, which allows deeper penetration through the different eye layers.[5]

The severity of symblephara ranges from subconjunctival inflammation and fibrosis to conjunctival forniceal obliteration, where the eyelid is completely adhered to the globe.[6] The fornix is required for ocular surface health by maintaining the tear reservoir, thus preventing dry eye disease, and it is the home for the accessory lacrimal glands. Symblephara may also cause ocular motility restriction, which may lead to double vision and headaches, as well as direct neuropathic pain. If left unchecked, symblephara may cause blindness due to dryness and tear insufficiency. When symblephara have formed, corneal decompensation and corneal transplantation often follow, the latter of which frequently fails due to an inadequate ocular surface environment to maintain a graft.[7] Current clinical treatments are ineffective to prevent or durably treat symblephara, and little is known about the molecular mechanisms behind their formation. An anti-adhesion therapy that inhibits the formation of symblephara would revolutionize how patients with ocular injuries are treated.[8]

Ocular surface alkali injury has been used to study corneal injury in mice[9–14]; however, the formation of symblephara in these mice has not been explored thus far. An alkali injury model described the formation of ocular symblephara in rabbits.[15] The rabbit ocular surface was injured with 2N NaOH for 90 seconds, and forniceal shortening and the formation of symblephara followed for 4 weeks. Although this model is useful for developing a basic understanding of the formation of symblephara, it may be difficult and expensive to use for high-throughput studies for testing therapeutics, with a long timeline until the formation of symblephara.

Years ago, the formation of symblephara after alkali burns in patients was treated with a glass rod to manually break the adhesion strands[16]; however, this approach was ultimately found to be ineffective at keeping the conjunctival surfaces sufficiently apart to prevent the reoccurrence of symblephara. Current treatment methods for alkali ocular burns include lamellar keratoplasty along with amniotic membrane transplantation (AMT) and autologous conjunctival or oral mucosal transplantation,[17,18] AMT with symblephara ring,[19] and soft contact lenses to keep the palpebral and bulbar surface apart.[16] However these methods are not completely effective because they may not reach the deep fornix region, where the conjunctiva can still adhere and cause forniceal shortening. Therefore, there is a need for alternative, more effective methods to prevent ocular adhesions. We describe

the first, to our knowledge, murine alkali-injury model that develops symblephara within 7 days. We also test a novel supramolecular polymer nanoparticle (PNP) hydrogel[20,21] that prevents conjunctival adhesions and forniceal shortening after alkali-burn injury in mice.

Methods

Animals

All experimental protocols were approved by the Stanford University Institutional Animal Care & Use Committee (APLAC #33501), and all procedures were conducted in accordance with the ARVO Statement for the Use of Animals in Ophthalmic and Vision Research and in compliance with the Animal Research: Reporting of In Vivo Experiments guidelines. C57BL6 male mice between the ages of 3 and 6 months were used for this study. Age-matched littermates were used for comparison. Experiments were repeated at different ages with similar results.

NaOH Dose Response

The mice were divided into five groups, each treated with increasing NaOH concentrations. Round filter papers disks (3.5-mm diameter) were soaked in 0, 0.25N, 0.5N, 1N, and 2N NaOH. They were subsequently placed under the superior and inferior mouse eyelids. The eyes were closed shut for 2 minutes, after which the filter paper was removed, the eyes were irrigated with phosphate-buffered saline (PBS), and pH was measured using pH test strips (M1095350001; MilliporeSigma, Burlington, MA) after absorbing excess PBS with a cotton sponge. Irrigation with PBS was continued until the pH measured 7.0.

Formation of Symblephara Over Time

Mice were divided into four groups, each treated with 1N NaOH as described above. The mice were allowed to recover and observed for 7 days. The globes and eyelids were together enucleated from the orbit by cutting around eyelid and under the eyeball such that the fornix structure was preserved. Tissue resection was done at days 1, 5, 7, and 14 after injury; fixed in 10% formalin; and sectioned into 5-μm-thick sections for hematoxylin and eosin (H&E) staining analysis.

PNP Hydrogel Preparation

For PNP hydrogel preparation, first polylactic acid (PLA)–polyethylene glycol (PEG) and hydroxypropyl

methylcellulose (HPMC)-C_{12} were synthesized, and PEG–PLA was nano precipitated as described below.

PEG–PLA Synthesis

A procedure was followed and analyzed as described previously.[22] PEG (0.25 g, 4.1 mmol) and *N,N′*-dibutylurea (DBU; 10.6 mg, 10 mL, 1.0 mol% relative to lactic acid) were dissolved in dichloromethane (DCM; 1.0 mL). Lactic acid (1.0 g, 6.9 mmol) was dissolved in DCM (3.5 mL) with mild heating. The lactic acid solution was then added rapidly to the PEG/DBU solution and was stirred rapidly for 10 minutes. The PEG–PLA copolymer was then recovered from the reaction medium by precipitation from excess 50:50 mixture of cold diethyl ether and hexanes, collected by filtration, and dried under vacuum to yield a white amorphous polymer.

HPMC-C_{12} Synthesis and Characterization

HPMC (1.5 g) was dissolved in *N*-methylpyrrolidone (NMP; 60 mL) by stirring at 80°C for 1 hour. When the polymer had completely dissolved, the solution was heated to 50°C. A solution of 1-dodecylisocyanate (0.5 mmol, 10% dodecyl modification by weight) was dissolved in NMP (5 mL) and added to the reaction mixture followed by 150 μL of *N,N*-diisopropylethylamine as a catalyst. The solution was then stirred at room temperature for 16 hours. This solution was then precipitated from acetone, and the HPMC-C_{12} polymer was recovered by filtration, dialyzed within a 3.5-kDa cutoff dialysis bag for 3 days in water, and then lyophilized, yielding a white amorphous material.

PEG–PLA Nanoprecipitation

A procedure was followed and analyzed as described previously.[22] A solution (1 mL) of PEG–PLA in acetonitrile (50 mg/mL) was added dropwise to water (10 mL) at a stir rate of 600 rpm. Nanoparticles were purified by ultracentrifugation over a filter with a molecular weight cutoff of 10 kDa (MilliporeAmicon Ultra-15 Centrifugal Filter Unit; MilliporeSigma) followed by resuspension in water to a final concentration of 250 mg/mL. Nanoparticle size and dispersity were characterized by dynamic light scattering (D_H = 35 nm, polydispersity index (PDI) = 0.02).

PNP Hydrogel Formulation

HPMC-C_{12} was dissolved in PBS at 6 wt% and loaded into a 1-mL Eppendorf tube. A 20 wt% PEG–PLA nanoparticle solution in PBS was then added to PBS and loaded into the tube. The HPMC polymer solution (150 mL) and nanoparticle solution (300 mL) were added together and mixed well by vortexing to create the PNP 1:10 hydrogel formulation.

PNP Hydrogel Treatment Regimen

The right and left eyes of each mouse were injured with 1N NaOH as described above. After irrigation and pH 7 was reached, 50 μL PNP hydrogel was applied on the ocular surface of the left eye and under the eyelid using a spatula. The right eye was left untreated. Eyelids were blinked so that the PNP hydrogel got evenly spread and reached the deep fornix of the eyes.

Histological Examination

For H&E-stained sections, 10% formalin fixed eyes were embedded in paraffin and 5-μm sections. Paraffin sections were deparaffinized using xylene and rehydrated in a graded series of ethanol and then water, and they were stained with H&E according to standard protocol. Images were taken on an EVOS XL Core Imaging System (Thermo Fisher Scientific, Waltham, MA) at 10× and 20× magnifications. For immunostaining, sections were blocked with 5% bovine serum albumin (BSA) in PBS for 1 hour, then incubated at 4°C overnight in primary antibody, alpha-smooth muscle actin (α-SMA) (C6198; Sigma-Aldrich, St. Louis, MO) or MSLN (250519; Abbiotec, Escondido, CA) diluted at 1:100 and 1:200, respectively, in 1% BSA in PBS. Sections were incubated in secondary antibody diluted at 1:250 for 1 hour, and nuclei were stained with 4′,6-diamidino-2-phenylindole (DAPI) for 5 minutes. Fluorescent images were taken using the THUNDER Imager EM Cryo CLEM microscope (Leica Microsystems, Wetzlar, Germany) at 10× and 20× magnifications. For Masson's trichrome and periodic acid–Schiff (PAS) stain, 5-μm sections were cut and stained according to the manufacturer's protocol. Quantitative analysis of collagen deposition and goblet cell numbers was done in Photoshop (Adobe, San Jose, CA).

Rheology Measurement and Fluorescent PNP Hydrogel Imaging

A 1:10 PNP hydrogel was used according to published methods.[20] Rheology measurements were performed on a DHR-2 rheometer (TA Instruments, New Castle, DE) using a 20-mm serrated plate geometry with a gap of 600 μm. Flow sweeps were performed at shear rates from 0.01 to 100 s^{-1}. Frequency sweeps were performed at a constant strain of 1% from 0.1 to 100 rad/s. dibenzocyclooctyne group (DBCO)-functionalized Alexa Fluor 647 dye (DBCO-AF647;

Jena Bioscience, Jena, Germany) was conjugated to azide-functionalized PEG–PLA nanoparticles through a copper-free click reaction. A 1.5× molar excess of dye to nanoparticle was added to the nanoparticle solution overnight at room temperature. The nanoparticles were then concentrated through centrifugation to remove any excess dye. To prepare the fluorescent PNP hydrogel, 50% dye-functionalized PEG–PLA nanoparticles were used in combination with 50% non-functionalized PEG–PLA nanoparticles. An in vitro imaging system, the Lumina Imager (PerkinElmer, Waltham, MA), was used to image fluorescent PNP hydrogel retention in the mouse eye. An exposure time of 0.1 second was used to quantify PNP hydrogel retention as the total flux of photons in the region of interest over time.

Statistical Analysis

Results in the figures represent mean ± SEM. Statistical analysis was done in Excel (Microsoft, Redmond, WA) and R (R Project for Statistical Computing, Vienna, Austria). Unpaired two-tailed Student's t-tests and one-way analyses of variance were performed to determine P values. Additionally, Kruskal–Wallis nonparametric tests were performed wherever indicated. $P \leq 0.05$ was considered significant.

Results

Conjunctival Injury With 1N NaOH Induced Forniceal Shortening and Formation of Symblephara in Mice After 7 Days

In control mouse eyes, the palpebral and bulbar conjunctiva line the eyelid and globe, respectively, forming the fornix at the junction (Fig. 1). The conjunctival fornix is required for ocular surface health. It provides a deep tear reservoir, allows smooth contact between the eyelid and globe, and permits full ocular motility. Alkali injury to the ocular surface causes forniceal shortening, leading to dry eye disease, formation of symblephara, and possible ocular motility restriction. To evaluate and test anti-scarring therapies for dry eye disease and symblephara, we first created a mouse conjunctival injury model using NaOH at increasing concentrations. The resulting conjunctival injury was evaluated based on the extent of forniceal shortening and conjunctival inflammation without globe destruction. Filter paper discs (3.5-mm) soaked in increasing NaOH concentrations of 0.25N, 0.5N, 1N, and 2N were placed under the mouse eyelids such that the bulbar and palpebral conjunctiva were in full contact with the soaked filter paper for 2 minutes. H&E-stained paraffin sections 7 days after injury showed no significant injury up to 0.5N NaOH (Figs. 2a–2c). At 1N NaOH, forniceal shortening was observed accompanied by conjunctival inflammation and increased immune cells at the injury site (Fig. 2d). At 2N NaOH, there was complete globe destruction after injury (data not shown). To determine the injury extent over time, we evaluated the mice at 1, 5, and 7 days after injury with 1N NaOH for 2 minutes (Fig. 3). There was minimal conjunctival injury in the H&E-stained paraffin sections after 1 day (Fig. 3a), such that the fornix and conjunctiva appeared normal. Five days after injury, the conjunctiva appeared damaged with adhesions between the palpebral and bulbar conjunctiva (Fig. 3b). Seven days after injury, the conjunctival adhesions were clearly evident, resulting in forniceal shortening, fibroblast infiltration, conjunctival inflammation, and fibrosis (Fig. 3c). Mice observed 14 days

Figure 1. The fornix joins the bulbar conjunctiva lining the globe with the palpebral conjunctiva lining the inside of the eyelid. The ciliary body, cornea, lens, and retina are shown for orientation.
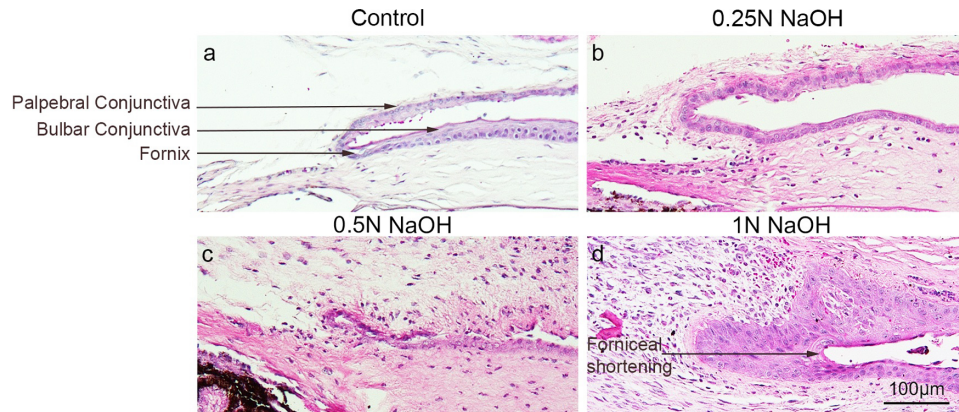
Figure 2. The 1N NaOH injury led to forniceal shortening and formation of symblephara. (a) H&E-stained paraffin-embedded sections of control mice with no injury and normal conjunctiva (*n* = 4). (b–d) H&E-stained section of mouse eyes injured with 0.25N NaOH for 2 minutes (*n* = 2) (b), 0.5N NaOH for 2 minutes (*n* = 2) (c), and 1N NaOH for 2 minutes (*n* = 6) (d).
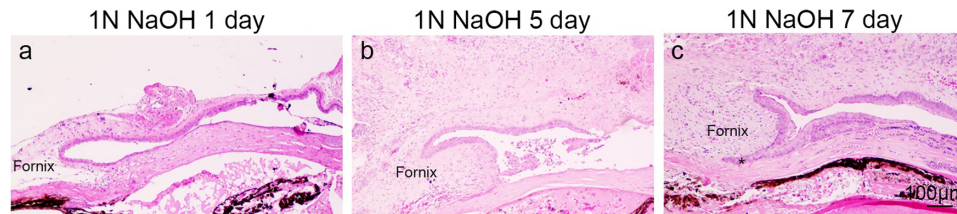

Figure 3. Forniceal shortening was maximum 7 days after injury. (a) Injury was minimal 1 day after 1N NaOH application (*n* = 2). (b) Five days after injury, conjunctival disruption and adhesion formation had begun (*n* = 3). (c) Seven days after injury, forniceal shortening and conjunctival adhesions were visible (*n* = 6).

after alkali injury showed globe destruction (data not shown); thus, 7 days was deemed the optimal formation time for symblephara.

PNP Hydrogel Prevented Forniceal Shortening After Alkali Injury

PNP hydrogels have proven to be an effective therapy for pericardial and abdominal fibrotic adhesions in rats and sheep following surgery.[20,21] The primary formulation evaluated in this study was comprised of 1 wt% of dodecyl-modified HPMC-C_{12} polymers and 5 wt% PEG–PLA nanoparticles ($D_H \sim 35$ nm), which is denoted as PNP-1-5. PNP hydrogels of different formulations exhibit tunable shear-thinning, self-healing, yield-stress, and viscoelastic properties that enable them to create a lubricious barrier between organs and tissues that reduces the incidence and severity of adhesions.[22–24] We have previously demonstrated that hydrogels that are too soft and weak flow too easily when perturbed in the body, leaving target tissues too quickly while adhesions are still developing. Hydrogels that are too stiff are easily dislodged from target tissues as the yield stress

of such materials exceeds their adhesion strength to the tissue. For these reasons, we sought to make use of modified HPMC as a functional polymer component, as this cellulosic derivative is known to be strongly muco- and tissue-adhesive.[20] Rheological characterization of PNP-1-10 hydrogels has demonstrated that these materials exhibit solid-like characteristics with G' > G'' across a broad range of frequencies, suggesting that they can form a robust barrier over the eye for significant timescales. At a frequency of 10 rad/s and 1% strain, the stiffness (G') of these materials was determined to be 13 Pa (Fig. 4a). These PNP-1-10 materials exhibited extreme shear thinning (3 orders of magnitude reduction in viscosity with increased shear rates), suggesting that these hydrogels can be easily spread over the eye by manual application (Fig. 4b). Additionally, the PNP hydrogel exhibits a functional yield stress, which is required for robust local persistence upon administration, as demonstrated by a flow sweep measurement where the stress was observed to asymptote to approximately 1 Pa at low shear rates (Fig. 4c).

To evaluate the anti-scarring and anti-fibrotic properties of the PNP hydrogel in the conjunctival adhesion mouse models as a preventative therapy
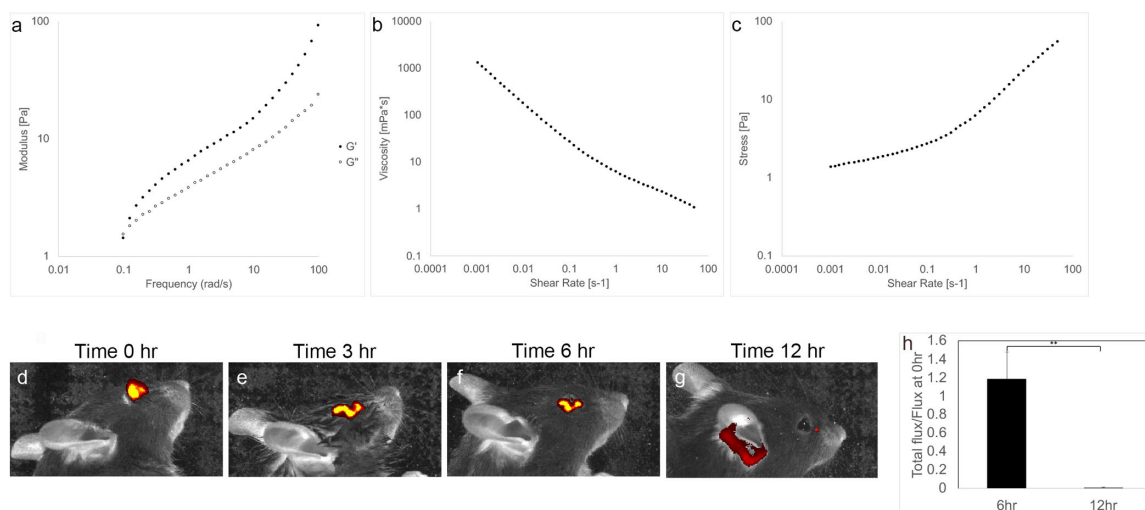
Figure 4. (a) Modulus to frequency of PNP hydrogel, (b) viscosity to shear rate, and (c) stress to shear rate showing solid versus liquid properties of the PNP hydrogel. Fluorescently labeled PNP hydrogel applied to the ocular surface and conjunctiva ($n = 3$) at 0 hours (d), 3 hours (e), 6 hours (f), and 12 hours (g). Epifluorescence scale bar is 0 to 3×10^9 radiant efficiency. (h) Quantification of total flux of fluorescently labeled hydrogel at 6 hours and 12 hours normalized to flux at 0 hour.

for symblephara, we tested fluorescently labeled PNP hydrogel at a 1:10 concentration in control mice. Fluorescently labeled PNP hydrogel was applied on the ocular surface and under the eyelids to form a barrier between the palpebral and bulbar conjunctiva at time 0 (Fig. 4d). In vivo imaging under the PerkinElmer IVIS fluorescent imaging system showed that fluorescent PNP hydrogel was present on the ocular surface at 3 hours (Fig. 4e) and 6 hours (Fig. 4f); however, by 12 hours (Fig. 4g), it was not detectable. Quantification of the region of interest at 6 hours and 12 hours showed a significant decrease in total flux (Fig. 4h).

To determine the efficacy of the PNP hydrogel in preventing conjunctival adhesions after alkali injuries, we applied the PNP hydrogel to the ocular surface and under the eyelids directly after 2-minute ocular surface injury with 1N NaOH. Seven days after injury, mice with the PNP hydrogel were compared to mice without PNP hydrogel 7 days after their injury (Figs. 5a–5e). As observed in H&E-stained sections, the injured mice that received PNP hydrogel had less severe adhesions and did not show forniceal shortening compared with injured mice without PNP hydrogel (Figs. 5f–5i).

Corneal injury after 1N NaOH injury, as observed by H&E-stained sections, was found to be more severe than after PNP hydrogel application (Figs. 5j–5o). Injured mice showed acute and chronic inflammatory infiltration, corneal edema, and loss of corneal clefts (Figs. 5k, 5n). Corneas with PNP hydrogel application showed milder corneal edema, as observed by corneal clefts and lesser inflammation in the anterior chamber.

PNP Hydrogel Did Not Prevent Conjunctival Goblet Cell Damage After Alkali Injury

Dry eye disease can be caused by alkali injury to the conjunctiva and from forniceal shortening. Conjunctival goblet cells produce mucins that keep the ocular surface hydrated and lubricated. To measure goblet cell damage after injury and to assess the protective potential of the PNP hydrogel, we stained paraffin-embedded sections with PAS, which stains mucin-producing conjunctival goblet cells (Fig. 6). Control mice conjunctiva showed healthy goblet cells stained in purple at the conjunctival epithelial surface (Fig. 6a). These goblet cells were absent from the badly damaged mouse conjunctivas from 2-minute injury with 1N NaOH for 7 days (Fig. 6b). PNP hydrogel application neither restored nor prevented goblet cell damage (Fig. 6c). PAS-stained goblet cell quantification showed no significant difference between goblet cell numbers in the injured compared with the PNP hydrogel–treated conjunctivas (Fig. 6d).

PNP Hydrogel Reduced Collagen Deposition, Myofibroblast Infiltration, and MSLN Expression After Alkali Injury

Collagen deposition is a hallmark of fibrotic disease. To determine the collagen deposition extent after injury, we performed Masson's trichrome staining, which turns collagen blue, on paraffin-embedded sections. Although collagen is intrinsically expressed
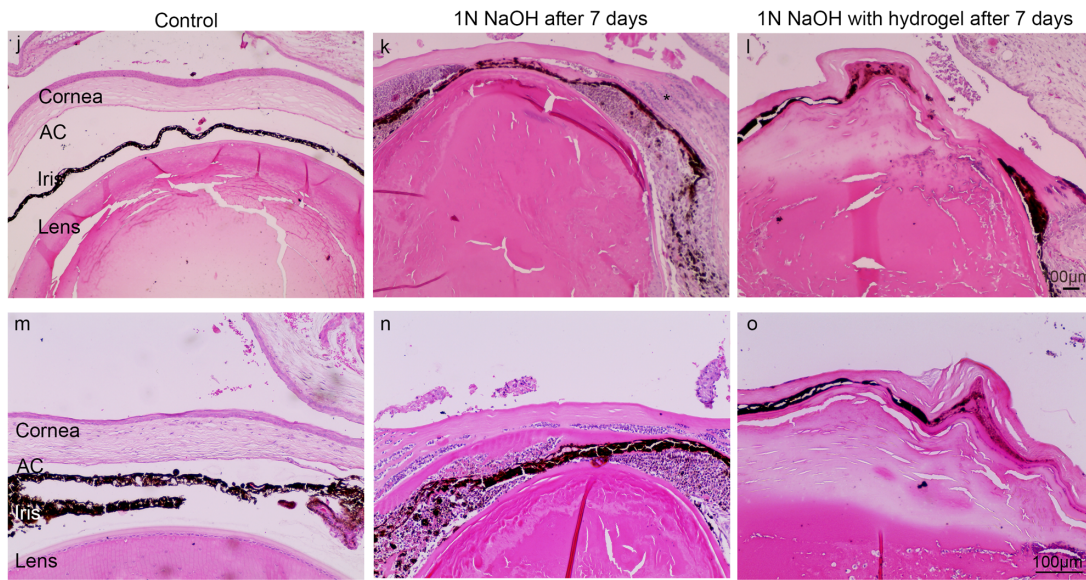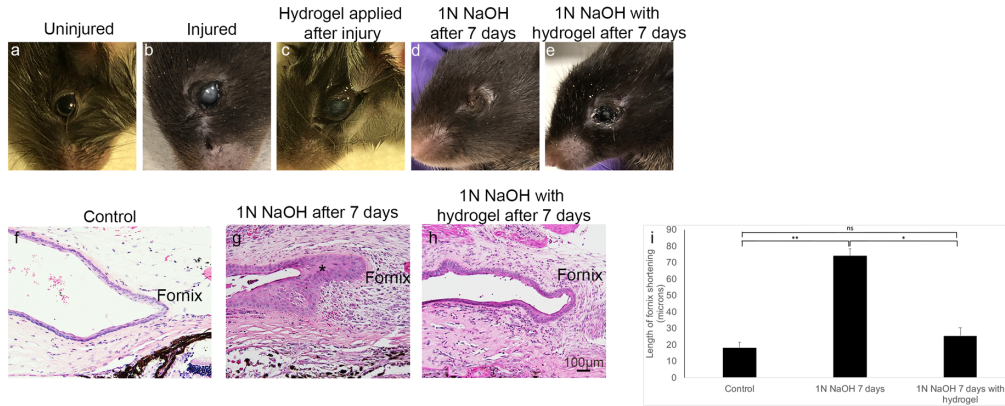
Figure 5. PNP hydrogel application after injury prevented forniceal shortening. (a) Control mouse with no injury ($n = 6$). (b) Mouse eye after injury with 1N NaOH for 2 minutes ($n = 6$). (c) PNP hydrogel applied to injured mouse eye immediately after injury ($n = 6$). (d) Injured mouse eye with no PNP hydrogel applied showed conjunctival adhesions and injury ($n = 6$). (e) Injured mouse eye with PNP hydrogel application showed less injury and fewer adhesions ($n = 6$). H&E-stained sections show the extent of injury with and without PNP hydrogel application. (f) Control mouse with no injury. (g) Mouse forniceal region 7 days after injury with 1N NaOH for 2 minutes (* indicates formation of symblephara). (h) Mouse forniceal region 7 days after injury with 1N NaOH for 2 minutes with PNP hydrogel application. (i) Quantification of forniceal shortening by measurement of distance of fornix end to fornix beginning ($n = 3$). (j) Control mouse cornea with no injury. (k) Mouse cornea 7 days after injury with 1N NaOH for 2 minutes (* indicates inflammatory cells). (l) Mouse cornea 7 days after injury with 1N NaOH for 2 minutes with PNP hydrogel application. Panels (m), (n), and (o) show control, 1N NaOH after 7 days, and 1N NaOH with hydrogel after 7 days, respectively, with corneas imaged at $20\times$ magnification ($n = 3$).
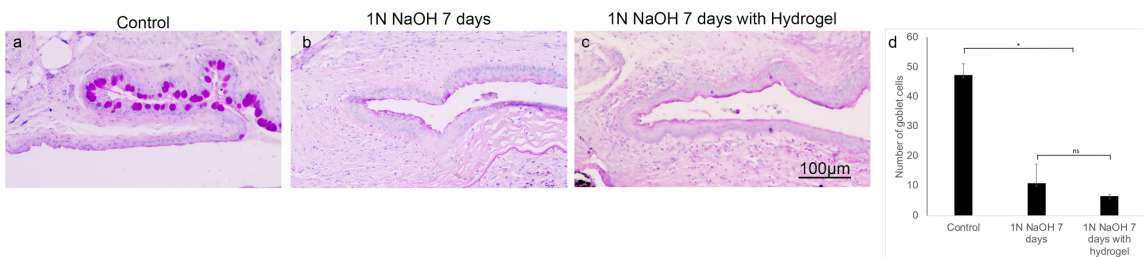

Figure 6. Goblet cells were destroyed after injury and with the PNP hydrogel. (a) Goblet cells stained with PAS in control mouse conjunctiva. (b) Goblet cells stained with PAS 7 days after injury with 1N NaOH for 2 minutes. (c) Goblet cells stained with PAS 7 days after injury with 1N NaOH for 2 minutes with PNP hydrogel application. (d) Quantification of number of PAS-positive cells staining goblet cells in the conjunctiva in control, injured, and injured with PNP hydrogel eyes ($n = 3$).
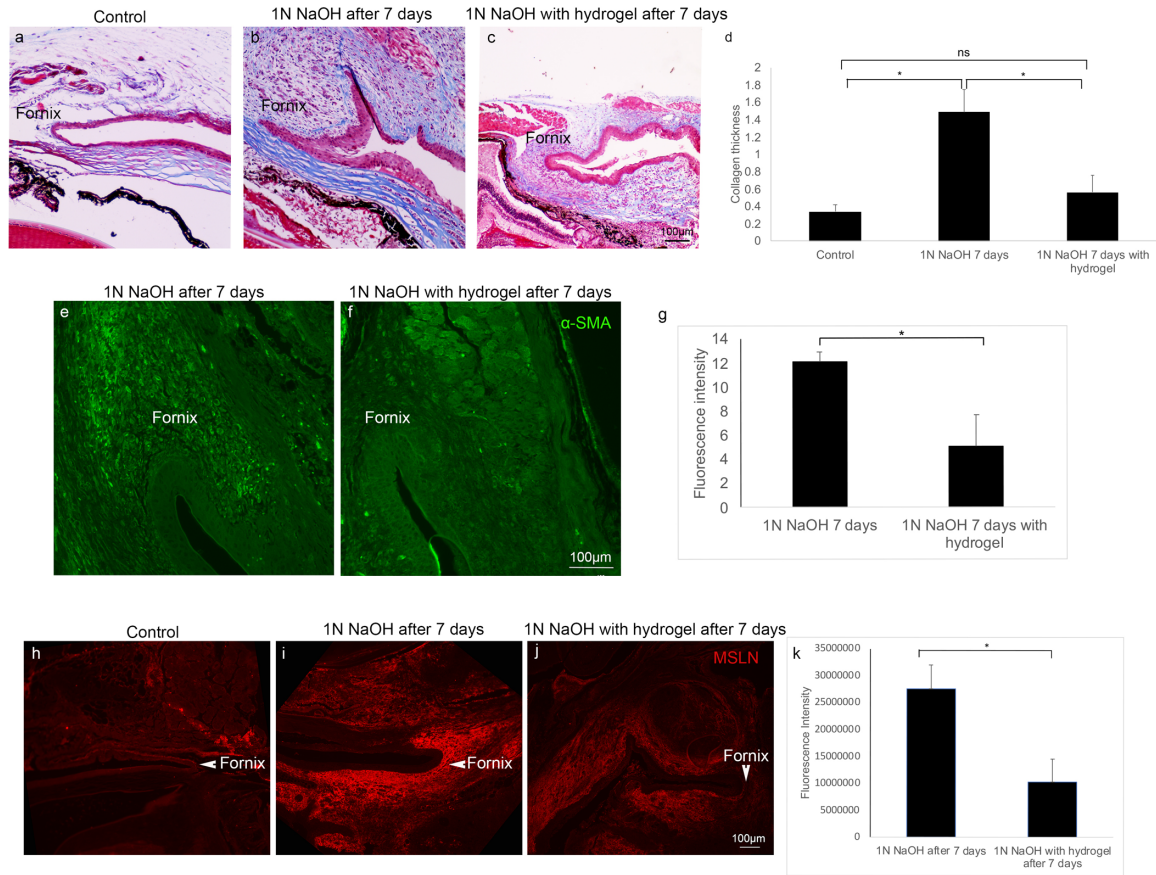
Figure 7. Masson's trichrome staining in blue showed more fibrotic collagen deposition in injured mice compared with injured mice treated with PNP hydrogel. (a) Control mice showing minimal blue staining collagen in the cornea. (b) Deposition of collagen in the forniceal region and immune cell infiltration in mice injured with 1N NaOH for 2 minutes. (c) Increase in immune cell infiltration in mice treated with PNP hydrogel but no conjunctival adhesions observed. (d) Quantification of collagen deposition by measurement of distance from fornix to levator palpebrae superioris shows a significant increase in collagen deposition in injured mice but not in injured mice treated with PNP hydrogel compared with control ($n = 3$). α-SMA as a myofibroblast marker at the site of injury: (e) α-SMA was upregulated in the forniceal region 7 days after injury with 1N NaOH for 2 minutes. (f) PNP hydrogel treatment ameliorated α-SMA expression and subsequent fibrosis. (g) Quantification of fluorescence intensity in injured and hydrogel-treated α-SMA stained tissue sections ($n = 3$). MSLN as a mesothelial marker at site of injury: (h) Control mouse eye stained with MSLN. (i) MSLN was upregulated in the forniceal region 7 days after injury with 1N NaOH for 2 minutes. (j) MSLN upregulation was relatively lower in eyes treated with PNP hydrogel. (k) Quantification of fluorescence intensity in injured and hydrogel-treated MSLN stained tissue sections ($n = 3$).

in mouse cornea, there is minimal collagen surrounding the forniceal region in control eye sections (Fig. 7a). Seven days after injury with 1N NaOH, collagen deposition was observed in the forniceal region along with fibroblasts (Fig. 7b). In paraffin sections from mice that were given topical PNP hydrogel after injury, there was less collagen deposition (Fig. 7c). Quantification of the distance from fornix to the levator superioris muscle in the Masson's trichrome–stained sections showed a significant increase in the collagen deposition in injured mouse tissue compared with control and PNP hydrogel–treated tissues. Additionally, we stained for the expression of α-SMA, which

is a myofibroblast marker at the injury site (Fig. 7d). We observed an increase in α-SMA–positive cell expression in the injured tissue that was lower in PNP hydrogel–treated tissues, indicating that fibrosis may be prevented by PNP hydrogel application (Figs. 7e–7g). To evaluate the potential mechanism of adhesion formation in the mouse alkali injury model, we stained the injury site with mesothelin (MSLN), a marker of mesothelial cells. We observed an increase in MSLN expression in the forniceal region with alkali injury compared with control (Figs. 7h, 7i), which was reduced in PNP hydrogel–treated eyes (Figs. 7j, 7k).

Discussion

Ocular surface alkali injury can lead to palpebral and bulbar conjunctival adhesions that form symblephara. To better understand how symblephara form and to evaluate preventive therapies, we have created an ocular conjunctival injury mouse model using NaOH. Alkali has been used to injure the cornea in mice[9,11,13]; however, these studies did not focus on the conjunctival effects as well as subsequent formation of symblephara. Prior studies have explored alkali injury on canine[25] and rabbit[26] conjunctiva using NaOH; however, genetic and therapeutic studies can be challenging in large animal models, in addition to the longer 4 to 5 weeks required for symblephara to develop. In our model, alkali injury caused the formation of symblephara with forniceal shortening without globe destruction within 7 days after injury. This finding provided a unique model for studying ocular alkali burns and cicatrizing conjunctival diseases and for evaluating preventative therapies. We also found that a novel topical PNP hydrogel can prevent forniceal shortening and the formation of symblephara up to 7 days after alkali injury.

An ideal animal model for symblephara should have tunable ocular surface injury without globe disruption and forniceal shortening due to adhesions.[26] One rabbit model of symblephara used a 10-mm filter paper crescent soaked in 2N NaOH for 90 seconds to induce symblephara.[26] In this study, symblephara formed in the late stages of alkali burns, around 4 weeks after NaOH injury, with fibroblast recruitment in the subconjunctival collagen fibers. Similarly, in a canine model of symblephara, symblephara formed 5 weeks after injury with 1N NaOH for 90 seconds.[25] In our mouse model, we observed forniceal shortening within 7 days of injury with 1N NaOH for 2 minutes. H&E and α-SMA stained tissue sections show fibroblast and myofibroblast infiltration at the injury site with eyelid margin deformation and crusting. The histological and molecular findings for mouse symblephara are similar to those for the rabbit and canine models, with the advantages that the symblephara form more quickly in mice and the ease of animal handling.

New symblephara preventive therapies would greatly benefit patients with alkali burns or cicatrizing disease. Previous studies have evaluated anti-adhesion materials made of cross-linked gelatin films,[27] sodium hyaluronate, and sesame oil[28] for their anti-inflammatory and anti-oxidative properties. Other studies have tested amniotic membrane and seprafilm as a barrier to prevent adhesions and symblephara.[19,29,30] Anti-adhesive materials have been mostly studied in the context of postoperative adhesions that form due to normal wound healing after surgery.

The molecular mechanisms involved in ocular adhesions are currently not well understood. JUN expression has been implicated in abdominal adhesions[31] where JUN was suppressed to prevent abdominal adhesions. Adhesions may form after mesothelial cell loss or damage at the injury site marked by MSLN and anti-MSLN antibodies.[32] MSLN has been explored as a therapeutic target for adhesion prevention. Although PNP hydrogel prevents the formation of symblephara after alkali injury, it may also prevent other cicatrizing diseases that involve ocular adhesions. We found an upregulation of MSLN after alkali injury, indicating that adhesion might originate due to loss of mesothelial cells at the site of injury. Our mouse model for symblephara may also be used to test molecular targets, such as JUN and MSLN, as the ocular surface contains mesothelial cells[33] that are involved in adhesion formation.

In the mouse model for symblephara, we found that PNP hydrogel prevented forniceal shortening. Although both of the products used clinically to prevent peritoneal adhesions, INTERCEED (Johnson & Johnson, New Brunswick, NJ) and Seprafilm (Baxter, Deerfield, IL), contain hyaluronic acid and carboxymethylcellulose,[34] these materials exhibit very poor performance, as they are easily dislodged from the site of administration.[20,34] Yet, Seprafilm was nevertheless found to be superior to polylactic acid, hyaluronic acid, chitosan, and PEG materials when evaluated in a rat cecum abdominal adhesion model.[35] In contrast, PNP hydrogels were found to be far superior to both INTERCEED and Seprafilm in rat and sheep models of abdominal and pericardial adhesions.[20,21] PNP hydrogels are composed of hydrophobically modified HPMC and PEG–PLA nanoparticles that imbue them with the unique ability to adhere to tissue surfaces, as demonstrated in rat and sheep models of postoperative adhesions.[20,21] In the present study, PNP hydrogels more easily reached the deep forniceal because of their superior tissue adherence and unique yield-stress and viscoelastic properties.[20,21] Furthermore, the PNP hydrogel shear-thinning and self-healing properties make them easy to handle and apply to the eye.

The presence of myofibroblasts (activated fibroblasts) is a key feature of pathological tissue repair and are upregulated in the conjunctival epithelial cells during fibrosis.[36] α-SMA is a myofibroblast marker expressed at the injury site.[37] α-SMA was significantly expressed in the forniceal region of our alkali-injury mouse model. This fits with other conjunctival injury models where

α-SMA was upregulated in the conjunctiva after injury.[38]

Collagen deposition is known to occur in fibrotic disease.[38,39] In the eye, collagen deposition after conjunctival injury has been observed in mice using allergic eye disease models[40,41] and a physical injury model[42] where collagen fibers were detected in the subconjunctival wounded area 7 days after injury. We observed collagen deposition in the alkali-injury mice with symblephara 7 days after injury which was reduced by treatment with PNP hydrogel. Goblet cell density was evaluated in a keratoconjunctivitis sicca mouse model[43] where goblet cells were reduced in the injured model, causing decreased mucoproteins. Goblet cells were almost completed ablated after alkali injury and were not protected by the PNP hydrogel, perhaps because they were immediately destroyed after NaOH application. Testing different PNP hydrogel concentrations may improve this effect in the future.

In conclusion, we describe, to the best of our knowledge, the first model for murine alkali-injury symblephara that can be useful for studying the pathophysiology of conjunctival scarring diseases. We tested a novel supramolecular PNP hydrogel that successfully prevents the formation of symblephara when applied after injury.

Acknowledgments

References

1. Brophy M, Sinclair SA, Hostetler SG, Xiang H. Pediatric eye injury-related hospitalizations in the United States. *Pediatrics*. 2006;117:e1263–e1271.
2. Wagoner MD. Chemical injuries of the eye: current concepts in pathophysiology and therapy. *Surv Ophthalmol*. 1997;41:275–313.
3. Haring RS, Sheffield ID, Channa R, Canner JK, Schneider EB. Epidemiologic trends of chemical ocular burns in the United States. *JAMA Ophthalmol*. 2016;134:1119–1124.
4. Eslani M, Baradaran-Rafii A, Movahedan A, Djalilian AR. The ocular surface chemical burns. *J Ophthalmol*. 2014;2014:196827.
5. Said DG, Dua HS. Chemical burns acid or alkali, what's the difference? *Eye (Lond)*. 2020;34:1299–1300.
6. Kheirkhah A, Blanco G, Casas V, Hayashida Y, Raju VK, Tseng SCG. Surgical strategies for fornix reconstruction based on symblepharon severity. *Am J Ophthalmol*. 2008;146:266–275.
7. Schonberg S, Stokkerman TJ. Ocular pemphigoid. *Ophthalmologe*. 2001;98:584–597.
8. Swarup A, Ta C, Wu AY. Molecular mechanisms and treatments for ocular symblephara. *Surv Ophthalmol*. 2021;67:19–30.
9. Hospital C, Qin H, Hospital C. Research on mouse model of grade II corneal alkali burn. *Int J Ophthalmol*. 2016;9:487–490.
10. Saika S, Ikeda K, Yamanaka O, et al. Therapeutic effects of adenoviral gene transfer of bone morphogenic protein-7 on a corneal alkali injury model in mice. *Lab Invest*. 2005;85:474–486.
11. Anderson C, Zhou Q, Wang S. An alkali-burn injury model of corneal neovascularization in the mouse. *J Vis Exp*. 2014;86:51159.
12. Ling S, Li W, Liu L, et al. Allograft survival enhancement using doxycycline in alkali-burned mouse corneas. *Acta Ophthalmol*. 2013;91:369–378.
13. Chen M, Gureeye AA, Cissé Y, Bai L. The therapeutic effects and possible mechanism of pranoprofen in mouse model of corneal alkali burns. *J Ophthalmol*. 2020;2020:7485912.
14. Herretes S, Suwan-Apichon O, Pirouzmanesh A, et al. Use of topical human amniotic fluid in the treatment of acute ocular alkali injuries in mice. *Am J Ophthalmol*. 2006;142:271–278.
15. Kang Y, Li S, Liu C, et al. A rabbit model for assessing symblepharon after alkali burn of the superior conjunctival sac. *Sci Rep*. 2019;9:13857.
16. Kaufman HE, Thomas EL. Prevention and treatment of symblepharon. *Am J Ophthalmol*. 1979;88:419–423.
17. Singh G, Bhinder HS. Evaluation of therapeutic deep anterior lamellar keratoplasty in acute ocular chemical burns. *Eur J Ophthalmol*. 2008;18:517–528.

18. Shi W, Wang T, Gao H, Xie L. Management of severe ocular burns with symblepharon. *Graefes Arch Clin Exp Ophthalmol*. 2009;247:101–106.

19. Ghaddar H, Teja S, Conlon R, Teichman J, Yeung S, Baig K. Ocular surface reconstruction with human amniotic membrane-symblepharon ring complex. *Can J Ophthalmol*. 2016;51:e129–e131.

20. Stapleton LM, Steele AN, Wang H, et al. Use of a supramolecular polymeric hydrogel as an effective post-operative pericardial adhesion barrier. *Nat Biomed Eng*. 2019;3:611–620.

21. Stapleton LM, Lucian HJ, Grosskopf AK, et al. Dynamic hydrogels for prevention of post-operative peritoneal adhesions. *Adv Ther*. 2021;4:1–9.

22. Grosskopf AK, Saouaf OA, Lopez Hernandez H, Appel EA. Gelation and yielding behavior of polymer–nanoparticle hydrogels. *J Polym Sci*. 2021;59:2854–2866.

23. Meis CM, Salzman EE, Maikawa CL, et al. Self-assembled, dilution-responsive hydrogels for enhanced thermal stability of insulin biopharmaceuticals. *ACS Biomater Sci Eng*. 2021;7:4221–4229.

24. Correa S, Grosskopf AK, Hernandez HL, et al. Translational applications of hydrogels. *Chem Rev*. 2021;121:11385–11457.

25. Tajiri K, Sugiyama T, Katsumura K, et al. Suppression of conjunctival scarring by chymase inhibitor in a canine symblepharon model. *Int J Ophthalmol Eye Sci*. 2016;S7:002:6–12.

26. Kang Y, Li S, Liu C, et al. A rabbit model for assessing symblepharon after alkali burn of the superior conjunctival sac. *Sci Rep*. 2019;9:13857.

27. Horii T, Tsujimoto H, Miyamoto H, et al. Physical and biological properties of a novel anti-adhesion material made of thermally cross-linked gelatin film: Investigation of the usefulness as anti-adhesion material. *J Biomed Mater Res B Appl Biomater*. 2018;106:689–696.

28. Khorshidi HR, Kasraianfard A, Derakhshanfar A, et al. Evaluation of the effectiveness of sodium hyaluronate, sesame oil, honey, and silver nanoparticles in preventing postoperative surgical adhesion formation. An experimental study. *Acta Cir Bras*. 2017;32:626–632.

29. Kara N. Sutureless amniotic membrane transplantation with a modified ocular surface ring. *Can J Ophthalmol*. 2018;53:e46–e48.

30. Shanbhag SS, Chodosh J, Saeed HN. Sutureless amniotic membrane transplantation with cyanoacrylate glue for acute Stevens-Johnson syndrome/toxic epidermal necrolysis. *Ocul Surf*. 2019;17:560–564.

31. Foster DS, Marshall CD, Gulati GS, et al. Elucidating the fundamental fibrotic processes driving abdominal adhesion formation. *Nat Commun*. 2020;11:4061.

32. Tsai JM, Sinha R, Seita J, et al. Surgical adhesions in mice are derived from mesothelial cells and can be targeted by antibodies against mesothelial markers. *Sci Transl Med*. 2018;10:eaan6735.

33. Jirsova K, Neuwirth A, Kalasova S, Vesela V, Merjava S. Mesothelial proteins are expressed in the human cornea. *Exp Eye Res*. 2010;91:623–629.

34. Ito T, Yeo Y, Highley CB, Bellas E, Benitez CA, Kohane DS. The prevention of peritoneal adhesions by in situ cross-linking hydrogels of hyaluronic acid and cellulose derivatives. *Biomaterials*. 2007;28:975–983.

35. Lin LX, Yuan F, Zhang H-H, Liao N-N, Luo J-W, Sun Y-L. Evaluation of surgical anti-adhesion products to reduce postsurgical intra-abdominal adhesion formation in a rat model. *PLoS One*. 2017;12:e0172088.

36. Shu DY, Lovicu FJ. Myofibroblast transdifferentiation: the dark force in ocular wound healing and fibrosis. *Prog Retin Eye Res*. 2017;60:44–65.

37. Aguilar X, Hallberg D, Sundelin K, et al. Myofibroblasts in the normal conjunctival surface. *Acta Ophthalmol*. 2010;88:407–412.

38. Sung MS, Eom GH, Kim SJ, Kim SY, Heo H, Park SW. Trichostatin a ameliorates conjunctival fibrosis in a rat trabeculectomy model. *Invest Ophthalmol Vis Sci*. 2018;59:3115–3123.

39. Seet LF, Toh LZ, Chu SWL, Finger SN, Chua JLL, Wong TT. Upregulation of distinct collagen transcripts in post-surgery scar tissue: a study of conjunctival fibrosis. *Dis Model Mech*. 2017;10:751–760.

40. Soriano-Romaní L, García-Posadas L, López-García A, Paraoan L, Diebold Y. Thrombospondin-1 induces differential response in human corneal and conjunctival epithelial cells lines under in vitro inflammatory and apoptotic conditions. *Exp Eye Res*. 2015;134:1–14.

41. Ahadome SD, Abraham DJ, Rayapureddi S, et al. Aldehyde dehydrogenase inhibition blocks mucosal fibrosis in human and mouse ocular scarring. *JCI Insight*. 2016;1:e87001.

42. Reichel MB, Cordeiro MF, Alexander RA, Cree IA, Bhattacharya SS, Khaw PT. New model of conjunctival scarring in the mouse eye. *Br J Ophthalmol*. 1998;82:1072–1077.

43. Dursun D, Wang M, Monroy D, et al. A mouse model of keratoconjunctivitis sicca. *Invest Ophthalmol Vis Sci*. 2002;43:632–638.